

Resolving Power of 2-D Pion Interferometry*

Sandra S. Padula¹ and Miklos GyulassyPhysics Department
Columbia University
New York, N.Y. 10027

November 21, 2018

Abstract: A χ^2 analysis is performed to test the resolving power of two-dimensional pion interferometry using for illustration the preliminary E802 data on $Si + Au$ at 14.6 AGeV/c. We find that the resolving power to distinguish two decoupling geometries of different dynamical models is enhanced by studying the variation of the mean χ^2 per degrees of freedom with respect to the range of the analysis in the q_T, q_L plane. The preliminary data seem to rule out dynamical models with significant ω, η resonance formation yields.

In this letter, the results of a new multi-dimensional pion interferometric analysis of preliminary E802 $\pi^-\pi^-$ correlation data[1]-[3] on central $Si + Au$ reactions at 14.6 AGeV/c are reported. To study the resolving power of multi-dimensional - in contrast to the projected one-dimensional interferometry - we consider two dynamical scenarios that predict similar correlation functions even though the underlying decoupling geometries differ considerably. We use the non-ideal inside-outside cascade model of Refs. [4, 5]. In one scenario long lived resonances are neglected while in the other the resonance fractions as taken from the Lund model. At higher SPS energies[4], we showed that long lived resonance production predicted by the Lund Model led to similar correlation functions to those expected from models with quark-gluon plasma formation[6], since long lived resonances could mimic the long slow burn of a plasma. Therefore another goal of the present study is to see if a similar ambiguity could exist at the lower AGS range. There is some fragmentary data[7] indicating that resonance production could be suppressed at the AGS, the Lund model predicts similar resonance yields at the two energy ranges. We show below that the two-dimensional χ^2 interferometric

⁰ *This work was supported by the Director, Office of Energy Research, Division of Nuclear Physics of the Office of High Energy and Nuclear Physics of the U.S. Department of Energy under Contract No. DE-FG02-93ER40764.

⁰ 1. Permanent address: IFT/UNESP, Rua Pamplona 145, 01405-900 São Paulo, SP, Brazil. Partially supported by Conselho Nacional de Desenvolvimento Científico e Tecnológico (CNPq), Brazil

analysis has sufficient resolving power to rule out significant long lived resonance production in the AGS domain, if the preliminary data are confirmed.

Recall that under idealized conditions the correlation function, $C_2(\mathbf{k}_1, \mathbf{k}_2)$, of two identical pions probes the decoupling or freeze-out space-time distribution of pions, $\rho(x)$, through $C_2(\mathbf{k}_1, \mathbf{k}_2) = 1 + |\rho(k_1 - k_2)|^2$. However, in actual high energy reactions, final state interactions, correlations between coordinate and momentum variables, and resonance production distort this ideal interference pattern due to Bose-Einstein symmetry (see e.g. [4]-[10]). The correlation function in this more general case can be expressed as[4]

$$C(k_1, k_2) = \Upsilon(q) \left(1 + \frac{|G(k_1, k_2)|^2}{G(k_1, k_1)G(k_2, k_2)} \right) , \quad (1)$$

where $\Upsilon(q) = (q_c/q)/(e^{q_c/q} - 1)$ is the Gamow factor that distorts the pattern due to Coulomb effects, with $q_c = 2\pi\alpha m$ and $q = -(k_1 - k_2)^2)^{1/2}$. The complex amplitude, $G(k_1, k_2)$, is the smoothed Fourier transform of the decoupling phase-space distribution $D(x, p) = \langle \delta^4(x - x_f) \delta^4(p - p_f) \rangle$, where (x_f, p_f) are the phase-space coordinates of the pions at their decoupling times x_f^0 . For minimum uncertainty Gaussian packets,

$$G(k_1, k_2) = \int d^4x d^4p D(x, p) e^{iqx} e^{q^2 \Delta x^2 / 2} e^{(p-K)^2 / 2 \Delta p^2} \propto \langle e^{iqx_f} e^{-Kp_f / \Delta p^2} \rangle , \quad (2)$$

where Δp is the rms momentum width of the packets. The interference pattern depends then not only on the break-up phase-space distribution, $D(x, p)$, but in general also on the quantal production dynamics characterized here by Δp . The standard notation $q = k_1 - k_2$ and $K = (k_1 + k_2)/2$ is used throughout. The distortions of the interference pattern due to long lived resonances modify the amplitude as [4].

$$G(k_1, k_2) \approx \langle \sum_r f(\pi^-/r) (1 - iqu_r / \Gamma_r)^{-1} \exp(iqx_r - Kp_r / \Delta p^2) \rangle , \quad (3)$$

where $f(\pi^-/r)$ is the fraction of the observed π^- 's arising from the decay of a resonance of type r , which freezes-out with final four velocity u_r^μ . The single inclusive pion distribution in this notation is $P_1(\mathbf{k}) \propto G(k, k)$. The Lund model in the AGS range suggests that $f(\pi^-/\omega) = 0.16$, $f(\pi^-/K^*) = f(\pi^-/(\eta + \eta')) = 0.09$, while some data seem to favor smaller fractions [7]. An aim of the present study is to test if multidimensional pion interferometry can discriminate between these possibilities.

We fit to the correlation data using the following parameterization of the break-up distribution[4, 5]

$$D(x, p) \propto \tau \exp \left\{ -\frac{\tau^2}{\Delta\tau^2} - \frac{(y - y^*)^2}{2Y_c^2} - \frac{(\eta - y)^2}{2\Delta\eta^2} - \frac{x_T^2}{R_T^2} \right\} \delta(E - E_p) \delta^2(\mathbf{p}_T) , \quad (4)$$

where $\tau = (t^2 - z^2)^{1/2}$ is the freeze-out proper time, and $\eta = \frac{1}{2} \log((t + z)/(t - z))$, $y = \frac{1}{2} \log((E + p_z)/(E - p_z))$ are the space-time and momentum rapidity variables. The correlation between these rapidities is estimated [4] from the Lund model to be $\Delta\eta \approx 0.8$.

The goal of the present interferometry analysis is to extract the rms transverse radius, R_T , at decoupling and the rms decoupling proper time interval, $\Delta\tau$. Note that unlike in

classical cascade models[11, 12], the transverse momentum in the above model is assumed to arise entirely from the finite momentum spread of the pion wave-packets through the parameter Δp . The $y^*, Y_c, \Delta p$ are fixed by fitting the single pion inclusive data[2] with

$$P_1(k) \propto G(k, k) \propto e^{-\frac{(y-y^*)^2}{2Y_c^2}} e^{-m_T/T} m_T^{-1/2}, \quad (5)$$

where $T = \Delta p^2/m$ is the effective transverse mass slope. We search for the optimal values of R_T and $\Delta\tau$ by fixing $\Delta\eta = 0.8$ from [4, 5] and $Y_c = 0.7$, $y_{cm}^* = 0$ and $\Delta p^2/m = 0.17$ GeV from the inclusive pion distributions[2]. Note that we assume implicitly that the chaoticity parameter $\lambda = 1$ in our analysis because, as we have emphasized in [4, 5], fits to data treating λ as a free parameter distort the geometrical scales in a further uncontrolled way.

For illustration, we recall that for special kinematics with $m_{1T} = m_{2T} = m_T$ and $\Delta y = y_1 - y_2$ small, the correlation function has the approximate analytic form when resonance production is neglected [5]

$$C(k_1, k_2) \approx 1 + \left\{ 1 + \frac{1}{2} m_T^2 \Delta\tau^2 \Delta y^2 (\Delta\eta^2 + \frac{Y_c^2 \Delta p^2}{\Delta p^2 + m m_T Y_c^2}) \right\}^{-2}. \quad (6)$$

This shows that the interference pattern as a function of the rapidity difference depends not only on the geometrical quantity of interest, $\Delta\tau$, but also on the width, $\Delta\eta$, of the $\eta - y$ correlation as well on the width, Y_c , of the finite rapidity distribution and on the wave-packets size.

To compare theoretical correlation functions with data projected onto two of the six dimensions, we must compute the projected correlation function

$$C_{proj}(q_T, q_L) = \frac{\int d^3 k_1 d^3 k_2 P_2(\mathbf{k}_1, \mathbf{k}_2) A_2(q_T, q_L; \mathbf{k}_1, \mathbf{k}_2)}{\int d^3 k_1 d^3 k_2 P_1(\mathbf{k}_1) P_1(\mathbf{k}_2) A_2(q_T, q_L; \mathbf{k}_1, \mathbf{k}_2)}, \quad (7)$$

where P_1 and P_2 are the one and two pion inclusive distributions, and A_2 is the experimental two pion binning and acceptance function. It is important to note that because of this projection, Coulomb corrections do not in general factor out of the integral. All calculation were performed using the Monte Carlo importance sampling method adopted in the CERES program[4, 5]. The acceptance function for the E802 experiment was approximated by

$$A_2(q_T, q_L; \mathbf{k}_1, \mathbf{k}_2) = A_1(\mathbf{k}_1) A_1(\mathbf{k}_2) \Theta(20 - |\phi_1 - \phi_2|) \delta(q_L - |k_{z1} - k_{z2}|) \delta(q_T - |\mathbf{k}_{T1} - \mathbf{k}_{T2}|). \quad (8)$$

The angles are measured in degrees and the momenta in GeV/c. The single inclusive distribution cuts are specified by

$$A_1(\mathbf{k}) = \Theta(14 < \theta_{lab} < 28) \Theta(p_{lab} < 2.2 \text{ GeV}/c) \Theta(y_{min} > 1.5). \quad (9)$$

To assess the statistical significance of the differences between the fits obtained assuming resonance and non-resonance dynamics, we compute the χ^2 goodness of fit on a two-dimensional grid in the (q_T, q_L) plane, binned with $\delta q_T = \delta q_L = 0.01$ GeV/c. In our preliminary analysis reported in Ref.[13], we compared the square of the difference between the

theoretical and experimental correlation functions and found an unexpected ridge of high variance along the $q_T = q_L$ diagonal. However, Zajc[14] pointed out that this feature could have been an artifact of statistical fluctuations in ratios of random variables, and suggested that the following χ^2 variable

$$\chi^2(i, j) = \frac{[A(i, j) - \mathcal{N}_\chi^{-1} C_{th}(i, j) B(i, j)]^2}{\{[\Delta A(i, j)]^2 + [\mathcal{N}_\chi^{-1} C_{th}(i, j) \Delta B(i, j)]^2\}} \quad (10)$$

should be used instead. In eq. (10), \mathcal{N}_χ is a normalization factor which is chosen to minimize the average χ^2 and depends on the range in the q_T, q_L plane under analysis. The indices i, j refer to the the corresponding q_T, q_L bins, in each of which the experimental correlation function is given by

$$C_{exp}(i, j) = \mathcal{N}_\chi \times \frac{A(i, j)}{B(i, j)} \quad ; \quad \Delta C_{exp}(i, j) = C_{exp}(i, j) \sqrt{\left(\frac{\Delta A(i, j)}{A(i, j)}\right)^2 + \left(\frac{\Delta B(i, j)}{B(i, j)}\right)^2} \quad (11)$$

The data for the numerator $A(i, j) \pm \Delta A(i, j)$ and denominator $B(i, j) \pm \Delta B(i, j)$ were obtained from R. Morse[3] with an understanding that the data in this form are preliminary and subject to further final analysis. We note that the published one-dimensional correlation data in [1] are not in a form suitable for our multi-dimesional analysis. Unfortunately, no final multi-dimesional correlation data are available at this time, and we use these data only for illustration of the method and to emphasize the need to go beyond traditional one-dimensional projections.

Minimization of the average χ^2 is performed by exploring the parameter space of R_T and $\Delta\tau$ and computing the $\langle\chi^2\rangle$, averaging over a 30x30 grid in the relative momentum region $q_T, q_L < 0.3$ GeV/c. In the vicinity of the minimum, $R_{T_0}, \Delta\tau_0$, we determine the parameters of the quadratic surface

$$\langle\chi^2(R_T, \Delta\tau)\rangle = \chi_{min}^2 + \alpha(R_T - R_{T_0})^2 + \beta(\Delta\tau - \Delta\tau_0)^2 \quad (12)$$

Recall that the average χ^2 over N bins is a random variable with unit mean and rms width $\sigma = \sqrt{2/N}$ if the $\chi(i, j)$ are normal random variables with zero mean and unit rms width. For large N , the distribution of the mean χ^2 per bin is $P(\chi^2) \propto \exp[-(\chi^2 - 1)^2/2\sigma^2]$. For the $N = 900$ grid under consideration, $\sigma \approx 0.047$.

The most direct measure of the goodness of the fit in this case is $n_\sigma = |\langle\chi_{min}^2\rangle - 1|/\sigma$, the number of standard deviations from unity of the average χ^2 per degree of freedom. Inserting eq. (12) into the asymptotic form of the χ^2 distribution for large N , the likelihood for the parameter R_T to have a value near the minimum is approximately $\propto \exp[-\alpha^2(R_T - R_{T_0})^4/2\sigma^2]$. We therefore estimate the error on the radius to be $\Delta R \approx \{\sqrt{2}[\Gamma(3/4)/\Gamma(1/4)]\sigma/\alpha\}^{1/2} \approx 0.7(\sigma/\alpha)^{1/2}$. Similarly, the estimated error on the proper time interval is $0.7(\sigma/\beta)^{1/2}$. The results of this statistical analysis are given in Table 1.

The lego plots of the Gamow corrected data and the corresponding theoretical correlation functions with and without resonances, corresponding to the optimized geometrical parameters, are shown in Figure 1 for the restricted range $0.005 < q_T, q_L < 0.125$ GeV/c. Part a) shows the 2-D data in the above range. Part (d) shows the corresponding experimental errors, which vary from $\Delta C \approx 0.1$ over most of this region to $\Delta C \approx 0.35$ toward the

right most corner at small q_T and large q_L . In part (b) the best fit (with $R_T = 4.6$ fm and $\Delta\tau = 3.4$ fm/c from Table 1 over the wider domain $q_T, q_L < 0.3$ GeV/c) assuming no resonance production is shown. In part (c) the best fit with Lund resonance fractions ($R_T = 3.1$ fm and $\Delta\tau = 1.6$ fm/c again over the wider range) is shown. Finally the $\chi^2(i, j)$ for the non-resonance scenario is shown in (e), whereas that corresponding to the full resonance fit is shown in part (f). Similar large fluctuations close to the edge of small q_T and large q_L is seen in both cases. However, the overall trend suggests that the no resonance fit is closer to the data in the region of small q even though the global χ^2 is about the same for both fits.

TABLE 1: 2D- χ^2 Analysis of Pion Decoupling Geometry

$\chi^2(R_T, \Delta\tau)$	No Resonances	LUND Resonances
E802 Data Not Gamow Corrected		
$\langle\chi^2_{min}\rangle$	1.125	1.128
R_{T_0}	4.1 ± 1.3	2.5 ± 1.3
$\Delta\tau_0$	3.3 ± 1.0	1.4 ± 1.0
α	0.014	0.013
β	0.021	0.023
E802 Data Gamow Corrected		
$\langle\chi^2_{min}\rangle$	1.098	1.104
R_{T_0}	4.6 ± 0.9	3.1 ± 1.3
$\Delta\tau_0$	3.4 ± 0.7	1.6 ± 1.0
α	0.027	0.014
β	0.042	0.023

The average χ^2 per degree of freedom depends, of course, on the range of q under analysis. We have tested this by varying the range of the analysis to restricted q_T, q_L domains, ranging from a 1×1 grid corresponding to $0.005 < q_T, q_L < 0.015$ GeV/c, to 2×2 , etc. as shown in Figure 2. However, instead of $\langle\chi^2\rangle$ we show there the number of standard deviations from unity of the averaged χ^2 per degree of freedom. For each $n \times n$ grid, $N = n^2$ is the number of degrees of freedom and the standard deviation is expected to be $\sigma = \sqrt{2}/n$. The strong dependence of the number of standard deviations from unity as a function of the range of the analysis is brought out clearly in Figure 2. We see that the optimal fit including Lund resonances is much worse than the fit without long lived resonance distortions when the analysis is restricted to the domain $q_L, q_T \leq Q_{max} \approx 100$ MeV/c, where the correlation function deviates significantly from unity. The two models yield similar acceptable fits in terms of χ^2 for $Q_{max} > 100$ MeV/c because in that large domain both predict models trivially predict nearly unit correlation functions. Also, the mean $\langle\chi^2\rangle$ begins to deviate strongly from unity for both models when data close to the edge of experimental acceptance, near $q_L, q_T \approx 0.3$ GeV/c, is included.

We conclude that multi-dimensional analysis has high resolving power in the domain of physical interest, and if these data are confirmed, the present analysis would rule out

long lived resonance production models in this energy range. However, we note that recent preliminary analysis in ref. [15] seems to give systematically lower correlation function values in the small q_T, q_L domain, in which case the resonance or an alternate long lived source geometry would be needed. In any case, the results show that 2-D χ^2 analysis can be used to improve considerably the resolving power of interferometry by amplifying in a quantitative way the differences between the data and calculations. We note that recent comparisons of interferometric data with cascade models, RQMD[11] and ARC[12], indicate good agreement with one-dimensional projected correlation data. However, the global χ^2 is quite poor. The study of the dependence of that χ^2 as a function of the range in those cases should help resolve where the models fail in a more quantitative fashion. Only in that case can one begin to assess whether the data are in fact consistent with standard hadronic transport models or require novel collective dynamics. In general, the analysis could be sharpened considerably by independent measurements of long lived resonance abundances to reduce that source of interferometric distortions.

Acknowledgements: We are grateful to R. Morse for his extensive help in making his unpublished data files and analysis available to us. Critical discussions with S. Nagamiya and W. Zajc are also gratefully acknowledged.

References

- [1] T. Abbott, et al (E802 Collab.), Phys. Rev. Lett. 69 (1992) 1030.
- [2] T. Abbott et al (E802 collab) Phys. Rev. Lett., 64 (1990) 847; Phys. Rev. Lett. 66 (1991) 1567.
- [3] R.J. Morse, MIT thesis 1990, Nucl.Phys. A525 (1991) 531c ; W. Zajc, Proc. QM91.
- [4] M. Gyulassy, S. S. Padula, Phys. Lett. 217B (1989) 181; S.S. Padula, M. Gyulassy, S. Gavin, Nucl. Phys. B329 (1990) 357.
- [5] S. S. Padula and M. Gyulassy, Nucl. Phys. B339 (1990) 378.
- [6] S. Pratt, Phys. Rev. D33 (1986) 1314; G. Bertsch, M. Gong, M. Tohyama, Phys. Rev. C37 (1988) 1896; Y. Hama, S. S. Padula, Phys. Rev. D37 (1988) 3237.
- [7] V. Blobel, et al, Phys. Lett. 48B (1974) 73.
- [8] G. F. Bertsch, Phys.Rev.Lett.72 (1994) 2349; G.F. Bertsch, P. Danielewicz, M. Herrmann, DOE-ER-40561-112, Sep 1993, in press.
- [9] S. Pratt, T. Csörgö, J. Zimanyi, Nucl. Phys. A527 (1991) 621c.; W. Bauer, C.K. Gelbke, S. Pratt, Ann. Rev. Nucl. Part. Sci. (1993), ed. J.D. Jackson, 77.

- [10] S. Chapman, P. Scotto, U. Heinz, TPR-94-29, Sep 1994, Act.Phys.Hun.: Heavy Ion Physics, in press.
- [11] J.P. Sullivan, M. Berenguer, D.E. Fields, B.V. Jacak, M. Sarabura, J.Simon-Gillo, H. Sorge, H. van Hecke, S. Pratt, Nucl. Phys. A566 (1994) 531c.
- [12] Y. Pang, T.J. Schlagel and S. Kahana, Phys. Rev. Lett. **68**, 2743 (1992).
- [13] M. Gyulassy and S. S. Padula, CU-TH-593 (93), Proc. of the HIPAGS '93 Workshop, MIT, Jan 13-15, 1993.
- [14] W. Zajc, Proc. of CAMP (LESIP IV), p. 439, ed. by M. Plümer, S. Raha and R. M. Weiner, World Scientific (1991).
- [15] R.A.Soltz, MIT thesis (1994) unpublished.

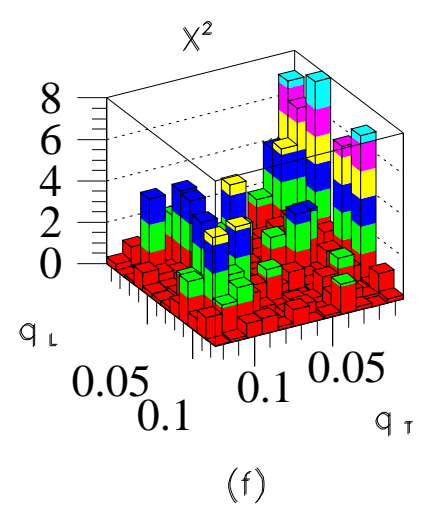
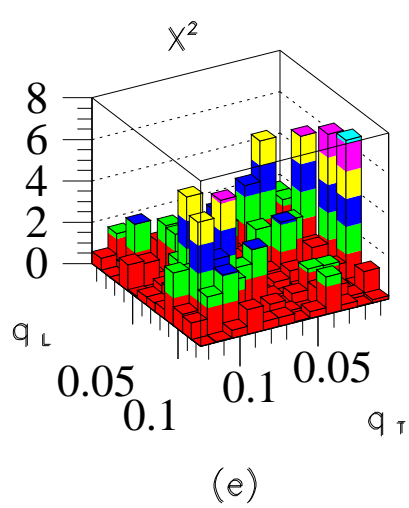
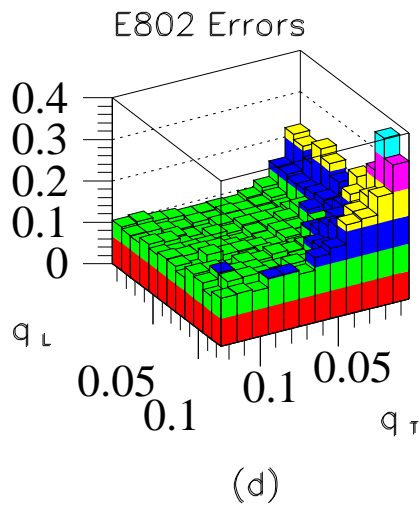
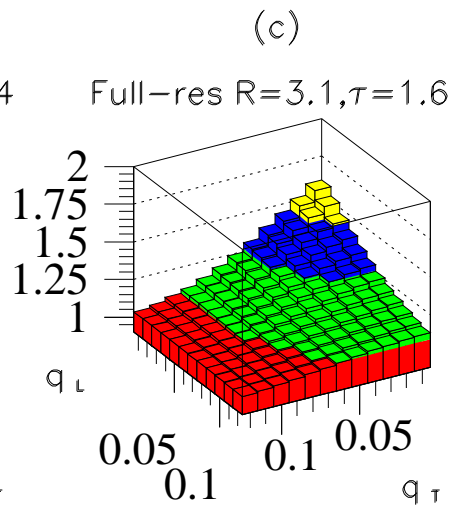
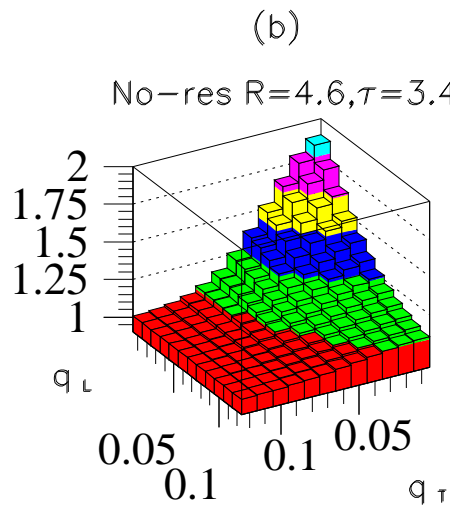
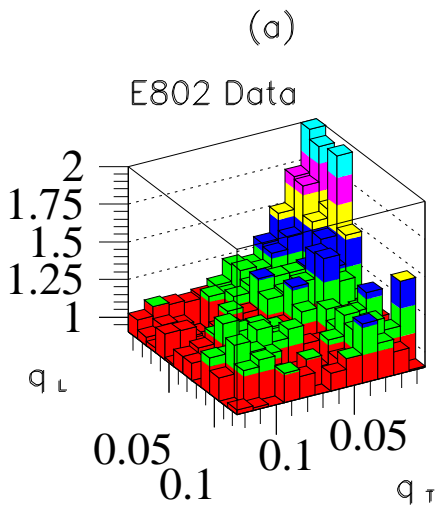
Figures Caption

Fig.1 Negative pion correlations in central Si+Au reactions[1] as a function of transverse and longitudinal momentum difference q_T, q_L . The preliminary E802 data corrected for acceptance and Coulomb effects are shown in part (a). Parts (b) and (c) show theoretical correlation functions filtered with the E802 acceptance for cases without and with resonance production, respectively. The transverse radius and proper time interval characterizing the pion decoupling distribution were obtained by minimizing the χ^2 over a wider region with $q_T, q_L < 0.3$ GeV/c. Part (d) shows the distribution of $\chi^2(q_T, q_L)$ for the case with resonance production in part (c). The average χ^2 parameters are listed in Table 1.

Fig.2 The number of standard deviations from unity of the χ^2 per degree of freedom as a function of the range Q_{max} of the analysis in the q_T, q_L plane.

This figure "fig1-1.png" is available in "png" format from:

<http://arxiv.org/ps/nucl-th/9501035v1>



This figure "fig1-2.png" is available in "png" format from:

<http://arxiv.org/ps/nucl-th/9501035v1>

Number of Standard Deviations from $\chi^2=1$

